Electronic Structure and Optical Properties of Charged Oligofluorenes Studied by VIS/NIR Spectroscopy and Time-Dependent Density Functional Theory

Silvia Fratiloiu,[†] Ferdinand C. Grozema,[†] Yoshiko Koizumi,[‡] Shu Seki,[‡] Akinori Saeki,[‡] Seiichi Tagawa,[‡] Stephen P. Dudek,[§] and Laurens D. A. Siebbeles*[,†]

Opto-Electronic Materials Section, DelftChemTech, Delft University of Technology, Mekelweg 15, 2629 JB Delft, The Netherlands, The Institute of Scientific and Industrial Research, Osaka University, 8-1 Mihogaoka, Ibaraki, Osaka 567-0047, Japan, and Laboratory of Macromolecular and Organic Chemistry, Eindhoven University of Technology, P.O. Box 513, 5600 MB Eindhoven, The Netherlands

Received: October 11, 2005; In Final Form: February 10, 2006

The electronic structure and optical properties of charged oligofluorenes were studied experimentally and theoretically. Measurements of the optical absorption spectra of charged oligofluorenes in dilute solutions have been performed by using the pulse radiolysis technique. In addition, optical absorption spectra of radical cations and anions in a solid matrix were measured after γ-irradiation at 77 K. The optical absorption spectra were measured in the range of 440−2100 nm (0.6−2.8 eV) and compared with results from time-dependent density functional theory (TDDFT) calculations. The calculated charge induced deformations and charge distribution do not indicate the occurrence of polaronic effects. The potential energy profiles for rotation around the inter-unit bond show that oligofluorenes are nonplanar in their neutral state, while they tend to more planar structures in their charged state. The optical absorption spectra of charged oligofluorenes are dependent on the angle between neighboring units. TDDFT absorption energies shift to lower values with increasing chain length, which suggests that the charge delocalizes along the oligomer chain.

1. Introduction

Conjugated polymers and oligomers offer an alternative to inorganic semiconductors for applications in optoelectronic devices, such as field-effect transistors (FETs),[1] light-emitting diodes (LEDs),[2] solar cells,[3] and nanoscale molecular electronic devices.[4] Semiconducting polyfluorenes[5] have been intensively studied in the last years for LED applications[6−9] due to their high fluorescence yield[10] and high charge carrier mobility.[11] Alkyl chains are introduced at the fluorene 9-position to induce polymer solubility, liquid crystallinity, and chirality without affecting the π-conjugated backbone. The applicability of fluorenes in LEDs critically depends on their charge transport properties. Radical cations and anions of fluorenes correspond to the charged species (holes and excess electrons) that are produced by charge injection from electrodes in a LED. Therefore the properties of charged fluorenes are of great interest. Optical absorption spectra of excess charges can provide valuable information about their spatial extent along the π-conjugated backbone.

Fluorene oligomers can be considered as model systems for conjugated polyfluorenes. For instance, the effect of chain length on the optical properties of charged oligofluorenes provides information about the delocalization of charge carriers, which can be extrapolated to the polymer. In the present study we report optical absorption spectra of positively and negatively charged oligofluorenes in dilute solution. Additional information on vibrational transitions in charged oligofluorenes was obtained by measuring the optical absorption spectra in a solid matrix at low temperature. Quantum chemical calculations were performed to gain insight into the nature of electronic transitions and into the spatial distribution of an excess charge. Quantum chemical calculations are an important tool to investigate the relation between the electronic structure and the optical properties of π-conjugated materials. The majority of the calculations reported in the literature describe neutral oligomers, while less work has been addressed to charged oligomers.[12−20] Most of the calculations performed on charged oligomers have been limited to semiempirical methods. Recently, time-dependent density functional theory (TDDFT) was used to calculate the optical absorption spectra of charged polycyclic aromatic hydrocarbons[16] and oligo(phenylenevinylene)s.[19,20] On the basis of the reported accuracy of this method to describe the lowest excited state of the charged systems,[16] we apply TDDFT to oligofluorene cations and anions. The experimental results in solution and solid matrix are compared with the calculated absorption spectra for oligomer chains with different length. The structures of the fluorene oligomers studied in this work are presented in Figure 1.

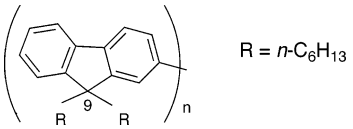

Figure 1. Chemical structure of the fluorene oligomers investigated. The optical absorption spectra of charged F*n* oligomers were measured in dilute solution, while the DHF*n* series was studied in solid matrix (*n* is the number of fluorene units).

2. Experimental Section

Experiments were performed on two series of fluorene oligomers with *n*-hexyl substituents at the 9-position (see Figure

* Address correspondence to this author. Phone: +31-15-278 1800. Fax: +31-15-278 7421. E-mail: l.d.a.siebbeles@tnw.tudelft.nl.
[†] Delft University of Technology.
[‡] Osaka University.
[§] Eindhoven University of Technology.

10.1021/jp055785f CCC: $33.50
Published on Web 03/09/2006

1). Both series of fluorene oligomers were prepared by similar synthetic strategies envolving step-by-step Suzuki cross-coupling reactions. The complete synthesis of the first series of fluorene oligomers (F*n*; *n* is the number of fluorene monomer units) has been published.[21] The second series of fluorene oligomers (DHF*n*; *n* is the number of fluorene monomer units) has been synthesized as reported earlier by Koizumi et al.[22] The details of the synthesis procedure are provided as Supporting Information.

F*n* solutions were prepared by using either UV-spectroscopic grade benzene (bz) or tetrahydrofuran (THF), depending on the nature of charges (positive or negative) to be studied. Solutions of F*n* in benzene were used for generating positive charges (F*n* radical cations), while the negative charges (F*n* radical anions) were created in THF. The benzene solutions (3 mM in monomer units) were bubbled with benzene-saturated oxygen for about 20 min. The tetrahydrofuran solutions (3 mM in monomer units) were bubbled with THF-saturated argon. The experiments on dilute solutions were carried out at room temperature.

Positive and negative charge carriers on isolated F*n* oligomers in solution were generated with pulse radiolysis. The F*n* solutions were irradiated with 5 ns pulses of 3 MeV electrons from a Van de Graaff accelerator. The positive and negative charge carriers were detected by time-resolved visible/near-infrared (VIS/NIR) spectroscopy, as reported previously for phenylenevinylene radical cations.[15,19] The absorption spectra of the F*n* radical cations and anions were measured by following the transient changes in absorbance of the solution at different wavelengths.

DHF*n* oligomers were dissolved in *n*-butyl chloride (BuCl) or methyltetrahydrofuran (MTHF) to study cationic and anionic species, respectively. The solutions (5−10 mM) were bubbled with dry argon for 2 min. Charge carriers were produced by γ-ray irradiation of DHF*n* solutions at 77 K with a dose of 4.0 kGy.[23] Optical absorption spectra of charged DHF*n* oligomers in solid matrix were recorded in the range 440−2100 nm at a temperature of 80−150 K, using a Shimadzu UV-3100PC spectrometer and an Oxford Optistat DN cryostat system.

3. Computational Methodology

The geometries of neutral and charged fluorenes were optimized by using the Amsterdam Density Functional (ADF) Theory program.[24] The geometry optimizations were performed by using the Local Density Approximation (LDA) with exchange and correlation functionals based on Vosko−Wilk−Nusair (VWN) parametrization of electron gas data.[25] The Generalized Gradient Approximation (GGA)[26] corrections by Becke[27] (exchange) and Perdew[28] (correlation) were included. For optimizing the geometries a double-ζ polarized (DZP) basis set was used.

The torsional potential energy profiles of neutral and charged bifluorenes were calculated with Density Functional Theory (DFT)[26] by taking the minimum energy conformation from the geometry optimization calculations and varying the interunit angle in steps of 15°. The geometry was not optimized for each angle. The DFT calculations were performed with the Q-Chem program,[29] using the Becke (exchange) and the Lee−Yang−Parr (correlation)[30] functional (BLYP), in a correlation consistent[31] polarized valence double-ζ (cc-pVDZ) basis set.

The optical absorption spectra of charged oligofluorenes were calculated with Time-Dependent Density Functional Theory (TDDFT),[32,33] as implemented in the Q-Chem program. The absorption energies were computed with use of the cc-pVDZ basis set and the BLYP functional.

In the calculations the alkyl chains at the 9-position were replaced by hydrogen atoms. This simplification is not expected to affect the optical spectra of the charged oligofluorenes significantly. The presence of the alkyl substituents does not create any significant steric effects[34] and should not affect the electronic transitions.

4. Results and Discussion

4.1. Measurement of Optical Absorption Spectra of Charged Fluorene Oligomers. Oligofluorenes (F*n*) in oxygen-saturated benzene ($[O_2] = 11.9$ mM at 1 atm and 25 °C) were irradiated with pulses of 3 MeV electrons from a Van de Graaff accelerator. This leads to the formation of benzene radical cations ($bz^{\bullet+}$), excited states (bz*), and excess electrons (e^-),[35−37] according to

$$bz \rightarrow bz^{\bullet+}, bz^*, e^- \quad (1)$$

The excess electrons generated during irradiation are highly mobile ($\mu = 0.13$ cm^2 V^{-1} s^{-1})[38] and react with the oxygen molecules (O_2) within a few nanoseconds, yielding oxygen anions (O_2^-).

$$e^- + O_2 \rightarrow O_2^- \quad (2)$$

The excited states of benzene molecules are quenched by O_2, leading to formation of O_2 in the $^1\Delta$ excited state.[39]

$$bz^* + O_2 \rightarrow O_2(^1\Delta) + bz \quad (3)$$

Benzene radical cations ($bz^{\bullet+}$) can react with the fluorene oligomers (F*n*) leading to the formation of fluorene radical cations ($Fn^{\bullet+}$).

$$bz^{\bullet+} + Fn \rightarrow bz + Fn^{\bullet+} \quad (4)$$

The occurrence of the reaction in eq 4 is evident from Figure 2a, which shows the change in optical absorption (ΔA) at 1920 nm (0.65 eV) due to formation of F3 cations upon irradiation. The absorbance at 1920 nm increases as reaction 4 proceeds. This reaction is possible due to the lower ionization potential of the fluorene oligomers as compared to benzene. The rate constant (k) for the diffusion-controlled reaction 4 can be calculated by using the relation

$$k = 4\pi RD \quad (5)$$

where R is the reaction radius and D is the diffusion coefficient. The diffusion coefficient can be calculated from the known mobility of holes in benzene ($\mu = 4 \times 10^{-4}$ cm^2 V^{-1} s^{-1}),[40] using the Einstein relation:

$$D = \frac{\mu k_B T}{e}. \quad (6)$$

Taking a typical reaction radius of 1 nm[41] and a monomer concentration of 3 mM the calculated rate coefficient ($k = 7.6 \times 10^9$ M^{-1} s^{-1}) corresponds to a rise time of the optical absorption signal near 50 ns, in agreement with the transient in Figure 2a. The decay of the transient absorption in Figure 2a on a time scale of hundreds of nanoseconds is attributed to second-order charge recombination.

$$Fn^{\bullet+} + O_2^- \rightarrow Fn + O_2 \quad (7)$$

A detailed discussion of diffusion-controlled reactions analogous

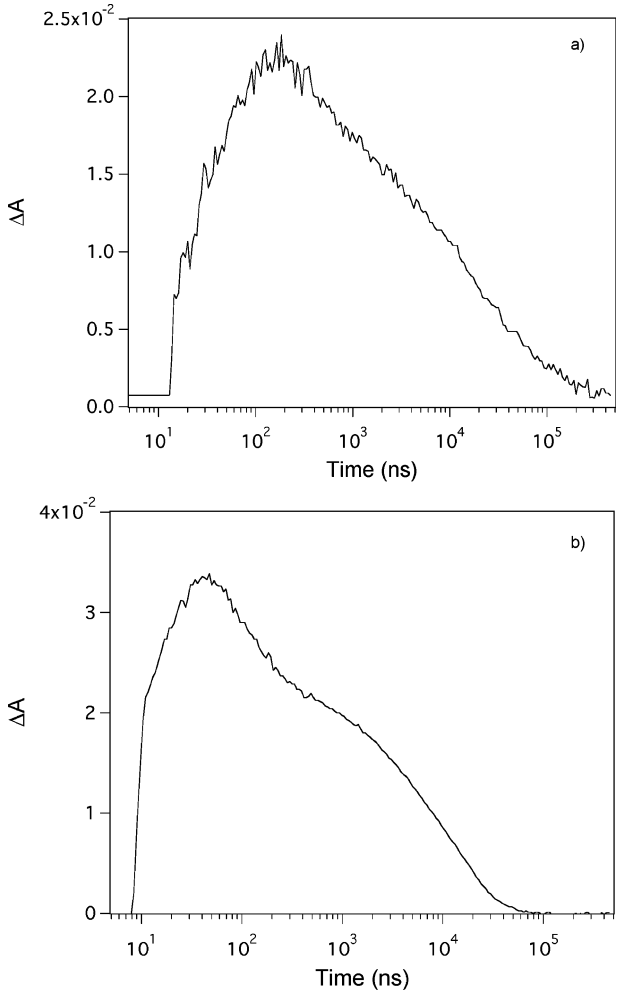

Figure 2. Optical absorption transients of F3 oligomers in solution at their maxima: (a) formation and recombination of F$n^{\bullet+}$ in O_2-saturated benzene and (b) formation and decay of F$n^{\bullet-}$ in Ar-saturated THF.

to those in eqs 2−4 and 7, describing the formation and recombination kinetics of positively charged species in solution, has been published previously.[42]

The optical absorption spectra of radical cations of fluorene oligomers (F*n*) in solution were measured in the range of 440−2100 nm (0.6−2.8 eV), see Figure 3 and Table 1. For the shortest radical cation (F1) the absorption was found to increase with the photon energy. However, the absorption maximum could not be observed in the accessible energy range and must thus occur at an energy above 2.8 eV. The spectrum of the F3 radical cation exhibits two absorption peaks at low energy (RC1) with maxima at 0.65 and 0.83 eV together with an absorption peak at high energy (RC2) (see Figure 3). Increasing the chain length from three to five fluorene units leads to one absorption peak at low energy (RC1), while no significant shift of the high-energy absorption peak (RC2) is observed. Data of the absorption maxima of the positively charged fluorene oligomers can be extended to data on polymers. Burrows et al.[43] have found the high-energy band (RC2) of the poly[9,9-di(ethylhexyl)-fluorene] radical cation at 2.2 eV. The RC2 energy of the F5 radical cation reported here (see Table 1) is similar to that of the polymer, indicating that the charged states in these systems saturate quickly.

To obtain the spectra of fluorene radical anions in solution, measurements were performed with tetrahydrofuran (THF) as a solvent.[44] Irradiation of THF leads to the formation of solvated electrons (e^-) and radical cations ($THF^{\bullet+}$), with a very small concentration of short-lived excited states.[45,46]

$$THF \rightarrow e^-, THF^{\bullet+}, THF^* \qquad (8)$$

Solvent radical cations ($THF^{\bullet+}$) react with neutral THF, according to[46,47]

$$THF^{\bullet+} + THF \rightarrow THF(-H)^{\bullet} + THF(+H)^+ \qquad (9)$$

Solvated electrons can undergo transfer to fluorene oligomers to form fluorene radical anions.

$$e^- + Fn \rightarrow Fn^{\bullet-} \qquad (10)$$

A small fraction of the solvated electrons is lost due to reaction with counterions (cations and radicals in THF).[46]

$$e^- + THF^+ \rightarrow THF^* \text{ (or THF)} \qquad (11)$$

$$e^- + THF(-H)^{\bullet} \rightarrow THF(-H)^{\bullet-} \qquad (12)$$

The formation and decay of the F3 radical anion can be observed in the optical absorption transient at 1620 nm in Figure 2b. The formation of F$n^{\bullet-}$ in tetrahydrofuran according to eq 10 occurs much faster than that of F$n^{\bullet+}$ in benzene (see eq 4) due to the fact that the electron mobility in THF ($\mu = 3 \times 10^{-3}$ cm V^{-1} s^{-1})[48] is much higher than the hole mobility in benzene (4×10^{-4} cm^2 V^{-1} s^{-1}).[40] If it is assumed that the reaction radius is 1 nm for the fluorene oligomer, a rate constant of 5.7×10^{10} M^{-1} s^{-1} is obtained, leading to a rise time less than 10 ns for a concentration of 3×10^{-3} mM (in monomer units), in agreement with the data in Figure 2b. The decay of the transient absorption in Figure 2b is attributed to the recombination of the fluorene radical anions with $THF(+H)^+$.

The optical absorption spectra of fluorene radical anions and cations are found to be similar, see Figures 3 and 4. No absorption was found for the F1 anion in the accessible wavelength range. The spectrum of the F3 radical anion exhibits two absorption maxima at low energy (RA1 and RA1′) and two maxima at high energy (see Figure 4 and Table 2). The maximum of the lowest energy band (RA1) is found near 0.7 eV. When the chain length of the fluorene anion is increased to five fluorene units (F5), there is only one maximum in the optical absorption spectrum at low energy (RA1), while two maxima appear at higher energy (see Figure 4).

From dosimetry measurements and pulse radiolysis data an estimation of the lower limit of the experimental extinction coefficients (ϵ) can be made, if it is assumed that all the charges generated during pulse radiolysis experiments react with the fluorene oligomers. The change in optical absorbance is related to the radiation dose, the yield of free charge carriers per unit dose (G), and the molar extinction coefficient (ϵ). The radiation dose per pulse was determined by dosimetry, using KSCN solution (10 mM) in N_2O-saturated water. For such a solution G and ϵ are accurately known ($G\epsilon(SCN)_2^- = 5.18 \times 10^{-4}$ m^2/J at 475 nm).[49] For the present optical experiments the radiation dose was determined to be 1.4 Gy per nC of beam charge and the yield of free charge carriers in benzene was taken from literature, $0.053(100\text{ eV})^{-1}$.[50] For experiments performed in THF the yield of free ions is $0.3(100\text{ eV})^{-1}$.[51] In this way the molar extinction coefficients were determined for both cations and anions of F*n* oligomers and they are listed in Tables 1 and 2.

Measurements of the optical absorption spectra were also performed for a second series of fluorene oligomers (DHF*n*) in a solid matrix after γ-irradiation, as described in section 2.

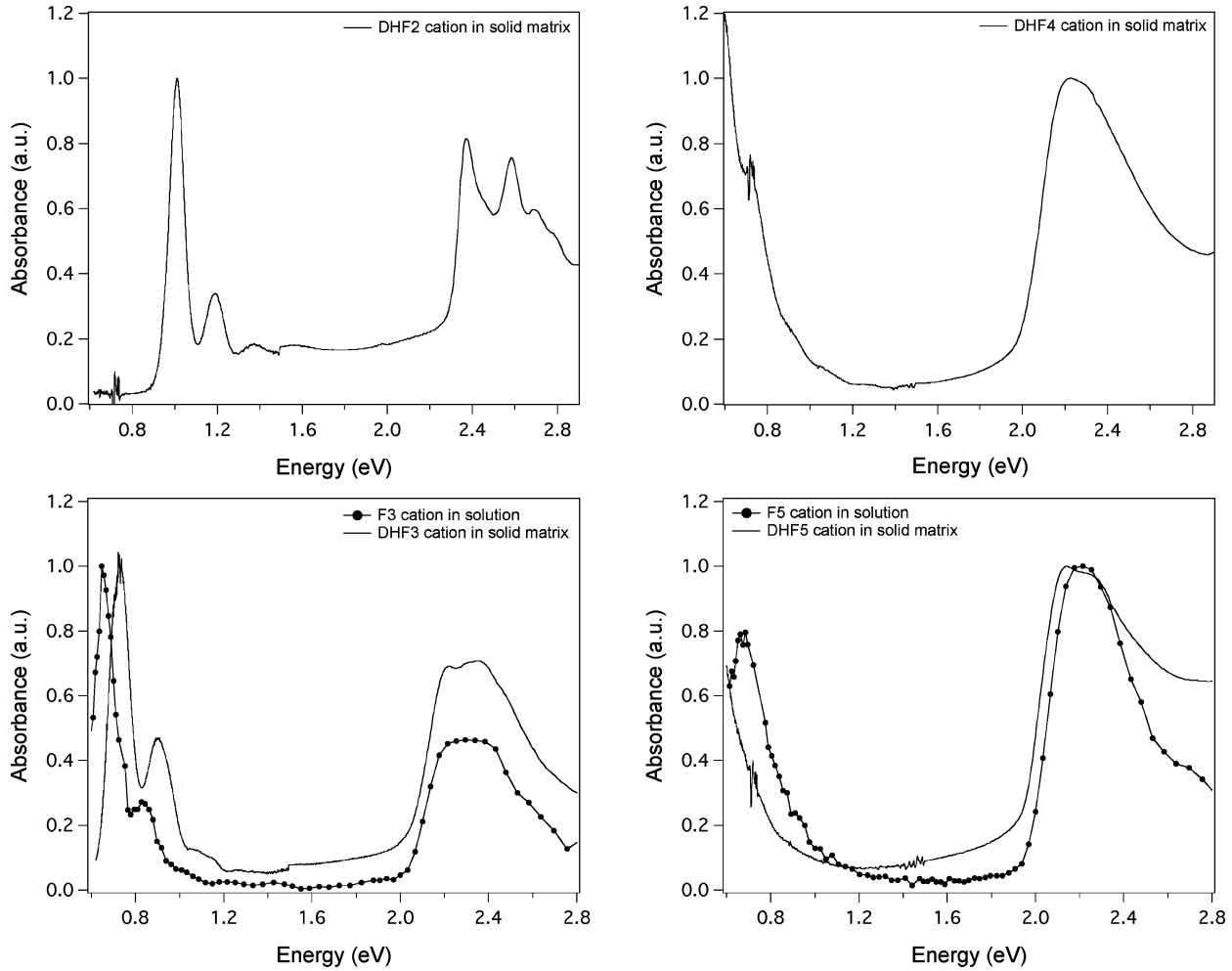

Figure 3. Optical absorption spectra of fluorene cations in solution (benzene) at room temperature together with the spectra in solid matrix (2-chlorobutane) at 100 K.

TABLE 1: Calculated and Experimental Transition Energies (ΔE), Experimental Extinction Coefficients (ϵ), Calculated Oscillator Strengths (f), and Composition of Excited States for Radical Cations of Fluorene Oligomers[a]

Fn	band	ΔE,[b] exptl eV	ΔE,[c] exptl eV	ϵ,[b] 10^4 L mol^{-1} cm^{-1}	ΔE calcd, eV	f	rel contribution of excited state configurations
F1	RC1	>2.8	2.05		2.18	0.11	−0.32(P1→P2) + 0.95(H-2→P1)
F2	RC1		1.01		1.24	0.45	1.01(H→P1)
			1.19				
	RC2		2.37		2.82	0.83	0.96(P1→P2) + 0.23(H→P1)
			2.58				
F3	RC1	0.65	0.73	9.0	0.85	0.79	1.08(H→P1)
		0.83	0.90	2.4			
	RC2	2.30	2.35	4.2	2.46	0.94	0.97(P1→P2) + 0.17(H→P1)
F4	RC1		<0.6		0.63	1.00	1.15(H→P1)
	RC2		2.23		2.30	0.88	0.96(P1→P2)
F5	RC1	0.67	<0.6	4.7	0.49	1.14	1.22(H→P1)
	RC2	2.21	2.14	5.9	2.22	0.84	0.96(P1→P2)

[a] Only transitions with oscillator strength higher than 0.1 are given. [b] Experimental data obtained from Fn spectra measured in solution. [c] Experimental data obtained from DHFn spectra measured in solid matrix.

Fluorene radical cations (DHF$n^{\bullet+}$) were produced by γ-irradiation of a frozen solution of DHFn in butyl chloride (BuCl) at 77 K. DHF$n^{\bullet+}$ is formed by charge transfer from mobile $BuCl^+$ to fluorene oligomers,[52] according to

$$BuCl \rightarrow BuCl^+, e^- \quad (13)$$

$$BUCl^+ + DHFn \rightarrow DHFn^+ + BuCl \quad (14)$$

$BuCl^-$ is not produced on irradiation because of the predominant dissociative electron attachment to the BuCl molecules.[52]

$$e^- + BuCl \rightarrow Bu^\bullet + Cl^- \quad (15)$$

Figure 3 shows the absorption spectra of radical cations of DHFn oligomers at 100 K. The spectrum of DHFn radical cations

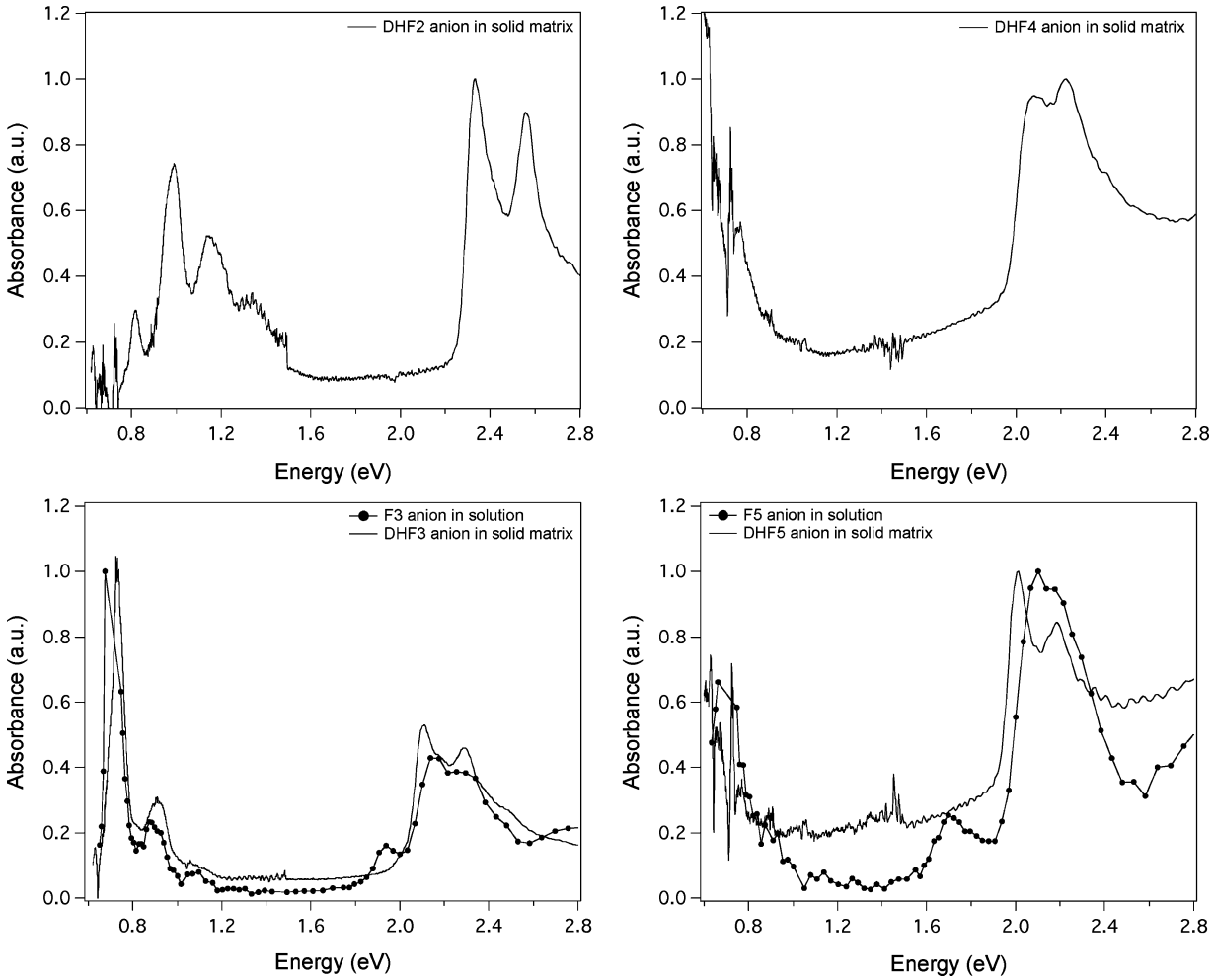

Figure 4. Optical absorption spectra of fluorene anions in solution (THF) at room temperature together with the spectra in solid matrix (MTHF) at 100 K.

TABLE 2: Calculated and Experimental Transition Energies (ΔE), Experimental Extinction Coefficients (ϵ), Calculated Oscillator Strengths (f), and Composition of Excited States for Radical Anions of Fluorene Oligomers[a]

Fn	band	ΔE,[b] exptl eV	ΔE,[c] exptl eV	ϵ,[b] 10^3 L mol^{-1} cm^{-1}	ΔE calcd, eV	f	rel contribution of excited state configurations
F1	RA1′				2.24	0.13	0.94(P2→L+2) − 0.33(P1→P2)
F2	RA1		0.82		1.24	0.34	−0.72(P2→L) − 0.61(P2→L+1)
			0.99				
	RA1′		1.14		1.48	0.14	0.28(P2→L) + 0.94(P2→L+2)
	RA2		2.33		2.74	0.94	0.21(P2→L) + 0.95(P1→P2)
			2.56				
F3	RA1	∼0.7	0.73	>10.6	0.83	0.44	0.85(P2→L) + 0.59(P2→L+2)
	RA1′	0.87	0.90	2.5	0.93	0.37	0.63(P2→L) − 0.80(P2→L+2)
	RA2	1.94	2.11	1.7	2.37	1.09	0.96(P1→P2)
		2.14	2.29	4.5			
F4	RA1		<0.6		0.65	1.05	1.12(P2→L)
	RA2		2.08		2.20	1.06	0.97(P1→P2)
			2.22				
F5	RA1	∼0.7	<0.6	>2.4	0.51	1.23	1.19(P2→L)
	RA2	1.70	2.01	0.9	2.13	0.97	0.97(P1→P2)
		2.10	2.18	3.6			

[a] Only transitions with oscillator strength higher than 0.1 are given. [b] Experimental data obtained from Fn spectra measured in solution. [c] Experimental data obtained from DHFn spectra measured in solid matrix.

exhibits absorption maxima at low energy and at high energy (see also Table 1), similar to the spectra measured in solution.

The formation of fluorene radical anions (DHF$n^{\bullet -}$) in γ-irradiated 2-methyltetrahydrofuran (MTHF) is attributed to attachment of electrons to oligofluorene molecules, analogous to experiments performed by Kira et al.[53]

$$e^- + \mathrm{DHF}n \rightarrow \mathrm{DHF}n^{\bullet -} \qquad (16)$$

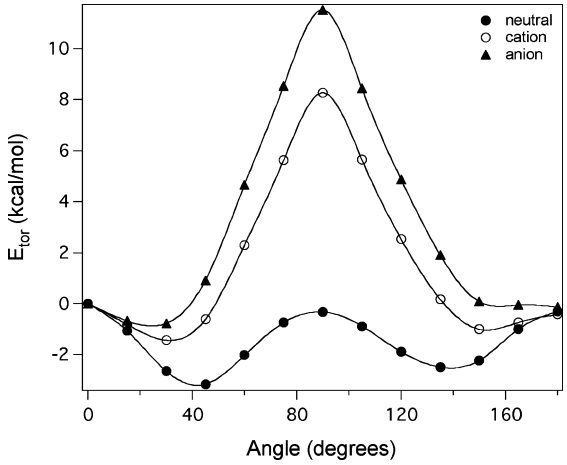

Figure 5. Potential energy profiles for torsional motion of the fluorene units. The zero point of the torsional energy (E_{tor}) is taken equal to the energy at zero torsional angle (θ_{tor}).

The optical absorption spectra of DHF*n* radical anions in solid matrix are similar to those measured in solution, see Figure 4 and Table 2.

4.2. Calculation of Geometry Deformations and Charge Distributions in Oligofluorene Cations and Anions. The geometries of neutral and charged oligofluorenes were optimized as described in section 3. It was found that oligofluorenes have a nonplanar structure in both neutral and charged states. Figure 5 shows the energies of neutral and charged bifluorenes as a function of the twist angle between the monomers, as calculated with DFT. The potential energy profile of neutral bifluorene has a minimum at an interunit angle of $\theta_{tor} = 41.6°$. A further twisting of the two fluorene units leads to less stable conformations, with a maximum energy close to $\theta_{tor} = 90°$. A second minimum of the torsional energy is found near $\theta_{tor} = 140°$. Our results agree with those of Belletete et al.,[34] who found a minimum energy for a torsion angle of 45.3°, using the Hartree−Fock method at the 6-31G* level. The potential energy surface of bifluorene is similar to that obtained for 1-(fluoren-2-yl)-phenylene by Tirapattur et al.,[54] which shows that an increase of the conjugation length does not affect the conformation of the molecule. From a geometry optimization of the neutral fluorene pentamer it was found that the optimum torsion angle between the fluorene units is between 40.4° and 41.4°. Thus, the interunit torsion angles do not change significantly with increasing conjugation length.

The potential energy profiles of the bifluorene cation and anion differ significantly from that for neutral bifluorene. The potential energy profile of the charged bifluorene has a minimum that corresponds to a conformation with an interunit angle of $\theta_{tor} = 31.7°$ for the bifluorene cation and $\theta_{tor} = 24.4°$ for the anion. Upon rotation around the interunit bond, the energy steeply increases to reach a maximum near $\theta_{tor} = 90°$ and then decreases to a second minimum around 150° and 160° for the bifluorene cation and anion, respectively.

The rotation barrier for neutral bifluorene is 2.9 kcal/mol. For charged bifluorenes the rotation barriers are much higher than those for neutral bifluorene: 9.7 kcal/mol for the cation and 12.4 kcal/mol for the anion, respectively. This leads to a more narrow distribution around the torsion angle for which the potential energy is minimum for the charged bifluorenes in comparison with the neutral molecule.

Information about the changes in C−C bond lengths when an electron is removed or added can be obtained by comparison of the optimized geometries of neutral and charged oligofluorenes. The changes in C−C bond lengths for the cations and anions of the fluorene dimer and pentamer are shown in Figure 6. The maximum change in C−C bond length was found to be 0.027 Å for both the bifluorene cation and anion (see Figure 6a). The C−C bond changes become smaller with increasing chain length: a maximum change of 0.01 Å for the F5 cation and 0.013 Å for the F5 anion, respectively (cf. Figure 6b). This can be understood in terms of the degree of charge delocalization. For longer chains the amount of charge per monomer unit is less and hence the geometry deformations are smaller. The geometry deformations, as obtained from DFT calculations, are spread over the oligofluorene chains with no indication of the formation of a self-localized polaron.

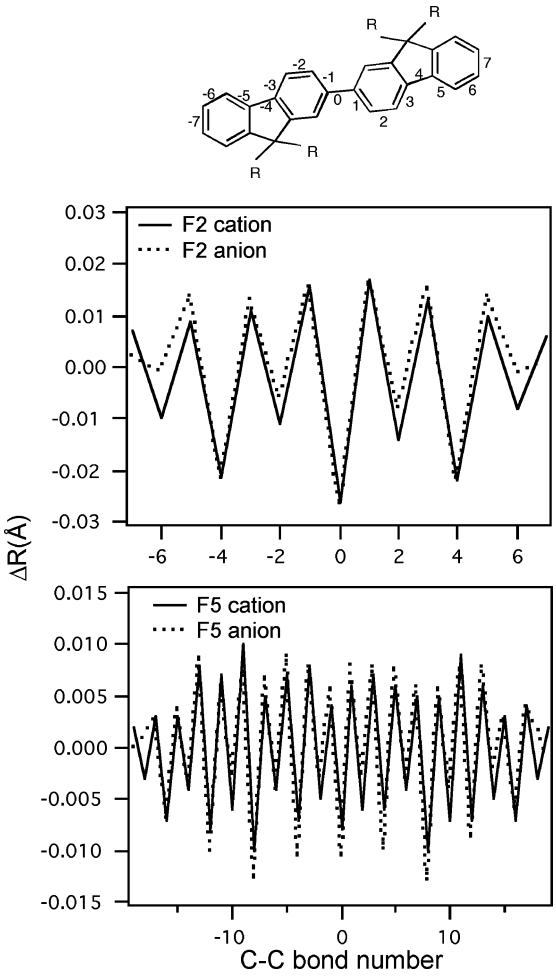

Figure 6. Changes in C−C bond length for the fluorene dimer and pentamer after removing or adding an electron as calculated with DFT. (The numbering of the bonds is indicated in the chemical structure.)

Information about the charge distribution along the oligomer chain is useful to gain insight into the occurrence of polaronic effects. Therefore, we have also analyzed the charge distribution of an excess positive and negative charge for the longest oligomer, F5 (see Figure 7). The charge distribution was obtained from a Mulliken population analysis performed with DFT. The charge distribution is presented in terms of fluorene units and was calculated as the difference between the charges of the atoms in the charged state and in the neutral state. The excess positive and negative charge of the F5 cation and anion, respectively, are delocalized along the chain. This means that no self-localized polaron is formed. Geometry deformations and charge distributions of phenylenevinylene cations and anions calculated with the DFT method were also found to be delocalized over the entire chain.[15,20]

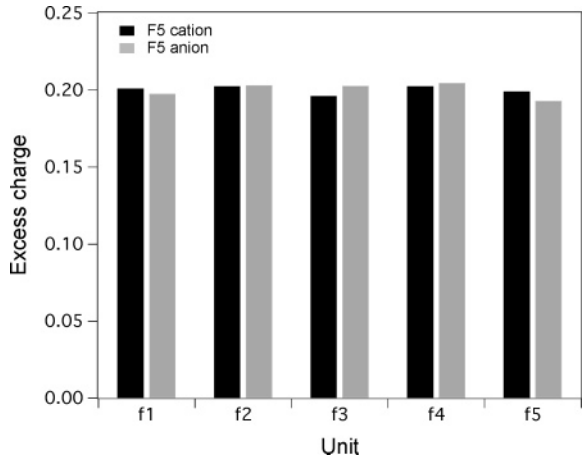

Figure 7. Distribution of an excess charge in F5 oligomer. Fluorene units are indicated as f*n* (*n*=1−5).

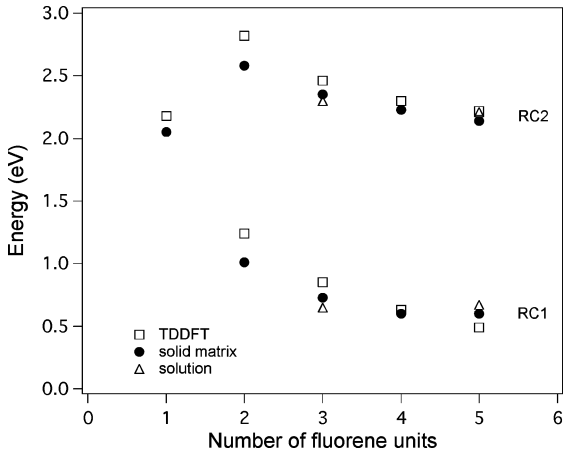

Figure 8. Chain length dependence of the transition energies for fluorene radical cations. The transition energies presented for the solid matrix correspond to the energies of the lowest RC1 transition (see Table 1) and the highest RC2 transition.

4.3. Comparison of Experimental and Calculated Optical Absorption Spectra of Charged Oligofluorenes. The absorption spectra of charged conjugated oligomers and polymers are usually explained in terms of the so-called "one-electron band structure model".[55,56] The model considers that the presence of a singly charged defect leads to the formation of two localized electronic levels in the gap between the valence band and the conduction band, the so-called polaron levels P1 and P2. Since oligomers have discrete energy levels instead of bands, the model was adapted to a "molecular orbital model" and it was presented previously for phenylenevinylene cations and anions.[15,20] According to this model, a positively charged system has the P1 level singly occupied, while P2 is empty. In a negatively charged system the situation is different: P1 is doubly occupied, while P2 is singly occupied. Note that P2 represents the lowest unoccupied molecular orbital (LUMO) for cations and the highest occupied molecular orbital (HOMO) for anions. According to this nomenclature, the level indicated as L is actually the second empty level for cations and the first empty molecular orbital (LUMO) for anions. The molecular orbital model was adopted in this study to describe the spectra of charged fluorenes.

4.3.1. Fluorene Cations. The optical absorption spectra of oligofluorene cations were calculated with the TDDFT method, as described in Section 3. The calculated transition energies are presented in Table 1 and Figure 8 together with the experimental data.

According to the TDDFT calculations there is only one allowed transition for the fluorene monomer in the energy range considered. This transition corresponds mainly to excitation of an electron from a doubly occupied molecular orbital (H-2) to the singly occupied molecular orbital (P1). From the experiments performed in solution the maximum of absorption could not be determined, while from the measurements on oligofluorenes in a solid matrix an absorption maximum was found at 2.05 eV, which is very close to the calculated energy of 2.18 eV.

When a second fluorene unit is added, two peaks appear at lower energy (1.01 and 1.19 eV) in the experimental absorption spectrum of DHF2 in a solid matrix of BuCl, in addition to the absorption features at higher energy (2.37 and 2.58 eV), see Figure 3. According to the calculations only a single electronic transition occurs at the lower energy. This suggests that the two peaks near 1 eV are due to different vibrational transitions with a spacing of ∼0.2 eV for the same electronic excitation. Infrared absorption and Raman spectroscopy[57] on fluorene indicate that several vibrational transitions occur near 0.2 eV, i.e., close to the energetic spacing between the peaks in the spectrum of the F2 cation. The TDDFT calculations predict only one electronic transition at higher energy (2.82 eV for the RC2 band in Table 1). This means that the absorption features at higher energy in the experimental spectrum (2.37 and 2.58 eV) correspond to two different vibrational transitions for the same electronic excitation.

For longer F*n* (n>2) cations the TDDFT absorption spectra exhibit two absorption bands: the RC1 band at an energy of 0.85 eV or lower and the RC2 band at energies just above 2.2 eV.

By inspection of the electronic configurations which dominate the calculated allowed transitions of the F*n* ($n > 1$) cations, it was found that the lowest transition (RC1) is dominated by excitation of an electron from the highest doubly occupied molecular orbital (H) to the singly occupied molecular orbital (P1). The second (RC2) transition corresponds mainly to excitation of an electron from the singly occupied molecular orbital (P1) to the lowest unoccupied molecular orbital (P2).

From comparison of the experimental and calculated transition energies in Table 1, it can be concluded that the experimental spectra of fluorene radical cations exhibit two absorption bands (RC1 and RC2), with different vibrational transitions for the same electronic excitation.

Analyzing the absorption energies of the F*n* cations as a function of the number of fluorene units in Figure 8, we can conclude that both the calculated RC1 and RC2 absorption energies decrease with increasing chain length. This can be understood as an increased delocalization of the charge with the number of fluorene units. The same behavior was found previously for phenylenevinylene[19] and thiophenevinylene[17] radical cations. The calculated red shift of the low-energy band with increasing chain length was also found in experiments performed on shorter oligofluorenes in a solid matrix. For the longer F*n* ($n = 4, 5$) cations in a solid matrix the RC1 band shifts to an energy below the instrumental lower limit of 0.6 eV, see Table 1 and Figure 3. In contrast, the energy of the RC1 band of fluorene cations in solution does not shift to lower energy on increasing the chain length from 3 to 5 fluorene units. This is attributed to a larger amount of disorder in the torsion angles between the fluorene units in solution, leading to a smaller average electronic coupling between the orbitals on the monomer units and hence a smaller energy change upon increasing the chain length.

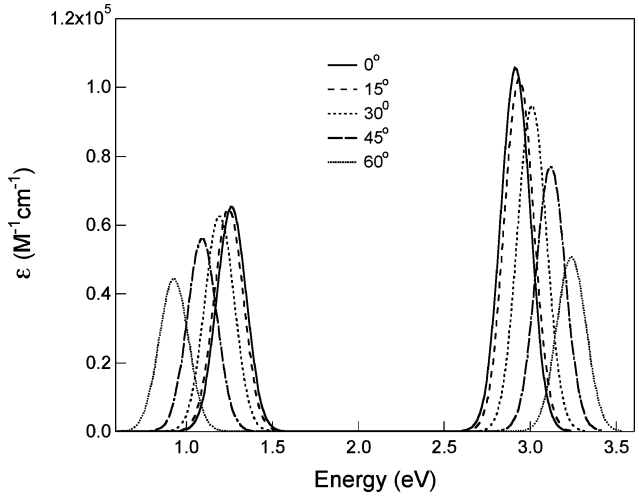

Figure 9. Angular dependence of the optical absorption spectra of the F2 cation. (The spectra were simulated by using a Gaussian distribution centered at the computed transition energy with an arbitrary width of 0.1 eV and an integrated amplitude equal to the computed oscillator strength.)

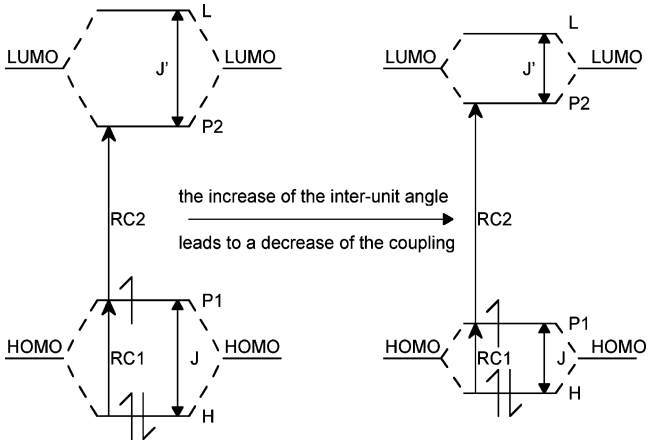

Figure 10. Molecular orbital model for oligofluorene cations, which explains the shifting of the absorption bands in Figure 9.

To study to what extent the interunit angle of the charged oligofluorenes affects their optical properties, the absorption spectrum of the bifluorene cation was calculated for different interunit angles. The angular dependence of the optical absorption spectrum of bifluorene cations is presented in Figure 9. The low-energy band (RC1), obtained by TDDFT, shifts to lower energies as the interunit angle increases, while the high-energy band (RC2) is blue shifted. This can be understood based on the molecular orbital model illustrated in Figure 10. The energies of the RC1 and RC2 electronic transitions are determined by the electronic couplings J and J' between the HOMO and LUMO orbitals, respectively, on the two fluorene monomers. It was found from the TDDFT calculations that the RC1 transition is dominated by an H → P1 excitation. The electronic coupling (J) decreases with increasing the interunit angle and becomes zero at 90°. This implies that the energy difference between H and P1 orbitals becomes smaller as the interunit angle (θ) increases. It can thus be concluded that an increase of the interunit angle (θ) of fluorene units leads to a decrease of the RC1 transition energy (see Figure 9). The RC2 electronic transition corresponds mainly to a P1 → P2 excitation. The electronic couplings J and J' decrease with increasing the interunit angle of the fluorene units. As a concequence the energetic difference RC2 between the P1 and P2 orbitals increases. Thus, the high-energy band (RC2) will be shifted toward higher energies, see Figure 9.

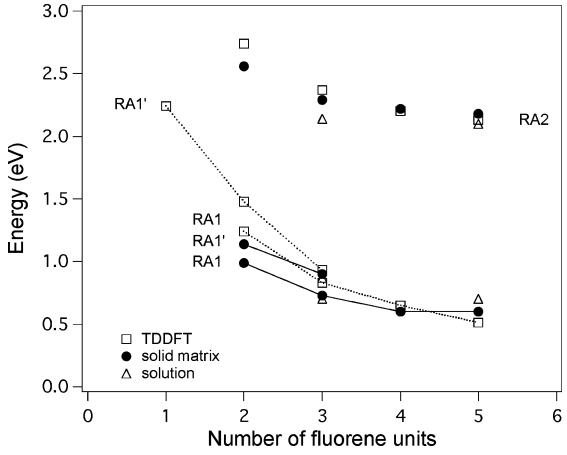

Figure 11. Chain length dependence of the transition energies for fluorene radical anions.

4.3.2. Fluorene Anions. Table 2 shows the calculated and experimental transition energies (ΔE) and the calculated oscillator strength (f) for fluorene anions. The chain length dependence of the transition energies of fluorene anions is shown in Figure 11. The RA1 transition energies, as calculated by TDDFT, shift to lower values with increasing chain length, which suggests that the charge delocalizes along the oligomer chain. The measurements performed on shorter Fn (n = 2, 3) oligomers in a solid matrix reproduce the red shift of the transitions at low energy with increasing the number of fluorene units. For the longer Fn (n = 4, 5) anions in a solid matrix the RA1 band exceeds the accessible experimental range toward lower energies. The chain length dependence of the lower absorption band RA1 of the negatively charged oligofluorene cannot be obtained from the measurements performed in solution.

As mentioned in section 4.1, no absorption band was observed for the monomer radical anion in solution or solid matrix. The TDDFT calculations yield an electronic transition at 2.24 eV in the absorption spectrum of the F1 anion. According to the calculations, this electronic transition is dominated by excitation of an electron from the singly occupied molecular orbital (P2) to the third empty molecular orbital (L + 2). Note that the calculated oscillator strength of the F1 electronic transition is very small (0.13 in Table 2) and could be below the experimental sensitivity.

A low-energy band consisting of different peaks (with maxima at 0.82, 0.99, and 1.14 eV) is observed for the fluorene dimer (DHF2) in solid matrix (see Figure 4). The TDDFT calculations on F2 give two electronic transitions at low energy (RA1 at 1.24 eV and RA1′ at 1.48 eV) and one at high energy (RA2 at 2.74 eV). Thus, according to the TDDFT calculations, the three well-resolved peaks at low energy in the experimental spectrum of the DHF2 anion can be attributed to two different electronic transitions (RA1 and RA1′) with the lowest electronic transition (RA1) having an additional vibrational transition. The lowest energy transition (RA1) was found to be dominated by excitation of an electron from the singly occupied molecular orbital (P2) to the lowest unoccupied molecular orbital (L). The second low-energy transition (RA1′) corresponds mainly to a P2 → L + 2 excitation, similar to that of the fluorene monomer anion. The high-energy transition (RA2) is dominated by a P1 → P2 excitation.

For the F3 radical anion both calculations and measurements yield two absorption bands at low energy (RA1 and RA1′).

According to the TDDFT calculations, there is only one electronic transition at higher energy (RA2). This means that the two absorption peaks from the experimental spectra of the F3 anion correspond to different vibrational transitions belonging to the same electronic excitation.

For longer F*n* ($n > 3$) radical anions the TDDFT calculations predict two electronic transitions, from which it can be concluded that the additional peaks in the experimental spectra are due to different vibrational transitions.

The data in Table 2 and Figure 11 show that the experimental transition energies of F*n* and DHF*n* anions are in general reproduced by the TDDFT calculations.

5. Summary and Conclusions

A combined experimental and theoretical study of the optical properties of charged oligofluorenes was carried out. Experiments were performed on oligofluorenes in solution and in a solid-matrix at low temperature. Positive and negative charges in solution were generated by irradiation with high-energy electrons from a Van de Graaff accelerator, while the charges in the solid-matrix were created by γ irradiation. The charged species were detected by VIS/NIR spectroscopy in the range of 0.6−2.8 eV. The experimental spectra exhibit distinct absorption bands at lower and higher energy with different vibrational transitions.

Quantum chemical calculations were performed on the cations and anions of oligofluorenes. The geometries of the charged oligofluorenes were optimized by using density functional theory (DFT). The geometry deformations and charge distribution were found to be delocalized along the entire oligomer chain without indication of polaron formation.

The optical absorption spectra of the charged fluorene oligomers were calculated with time-dependent density functional theory (TDDFT). Calculations performed for the charged fluorene dimer show that the optical absorption spectra are dependent on the interunit angle between the two-fluorene units. Therefore we have studied the potential energy profiles for rotation around the interunit bond. It was found that charged oligofluorenes have a much more planar structure than in the neutral state.

The TDDFT method predicts a monotonic decrease of the absorption energies with increasing chain length, which suggests an increased delocalization of the charge, as the oligomer chain becomes longer. The calculated monotonic decrease of the absorption energies is less pronounced in the measurements. The good agreement between the theoretical absorption energies and the experimental data for the charged oligofluorenes stimulates the application of the TDDFT method to other charged systems.

Acknowledgment. The authors acknowledge Dr. J. M. Warman and Dr. A. Krylov for valuable discussions and M. Vermeulen and R. D. Abellon for technical support. The Netherlands Organization for Scientific Research (NWO) is acknowledged for financial support by an NWO-VENI grant.

Supporting Information Available: Complete synthesis procedures. This material is available free of charge via the Internet at http://pubs.acs.org.

References and Notes

(1) Reese, C.; Roberts, M.; Ling, M.; Bao, Z. *Mater. Today* **2004**, *7*, 20.

(2) Kraft, A.; Grimsdale, A. C.; Holmes, A. B. *Angew. Chem., Int. Ed.* **1998**, *37*, 402.

(3) Brabec, C.; Dyakonov, V.; Parisi, J.; Sariciftci, N. S. *Organic Photovoltaics*; Springer: Berlin, Germany, 2003.

(4) Carroll, R. L.; Gorman, C. B. *Angew. Chem., Int. Ed.* **2002**, *41*, 4378.

(5) Scherf, U.; List, E. J. W. *Adv. Mater.* **2002**, *14*, 477.

(6) Leclerc, M. *J. Polym. Sci. Part A: Polym. Chem.* **2001**, *39*, 2867.

(7) Pogantsch, A.; Wenzl, F. P.; List, E. J. W.; Leising, G.; Grimsdale, A. C.; Mullen, K. *Adv. Mater.* **2002**, *14*, 1061.

(8) Kulkarni, A. P.; Jenekhe, S. A. *Macromolecules* **2003**, *36*, 5285.

(9) Gruber, J.; Li, R. W. C.; Aguiar, L. H. J. M. C.; Benvenho, A. R. V.; Lessmann, R.; Hummelgen, I. A. *J. Mater. Chem.* **2005**, *15*, 517.

(10) Belletete, M.; Ranger, M.; Beaupre, S.; Mario, L.; Durocher, G. *Chem. Phys. Lett.* **2000**, *316*, 101.

(11) Redecker, M.; Bradley, D. D. C. *Appl. Phys. Lett.* **1999**, *74*, 1400.

(12) Cornil, J.; Beljonne, D.; Bredas, J. L. *J. Chem. Phys.* **1995**, *103*, 834.

(13) Cornil, J.; Belijonne, D.; Bredas, J. L. *J. Chem. Phys.* **1995**, *103*, 842.

(14) Ottonelli, M.; Moggio, I.; Musso, G. F.; Comoretto, D.; Cuniberti, C.; Dellepiane, G. *Synth. Met.* **2001**, *124*, 179.

(15) Grozema, F. C.; Candeias, L. P.; Swart, M.; van Duijnen, P. T.; Wildeman, J.; Hadziiannou, G.; Siebbeles, L. D. A.; Warman, J. L. *J. Chem. Phys.* **2002**, *117*, 11366.

(16) Hirata, S.; Head-Gordon, M.; Szczepanski, J.; Vala, M. *J. Phys. Chem. A* **2003**, *107*, 4940.

(17) Grozema, F. C.; van Duijnen, P. T.; Siebbeles, L. D. A.; Goossens, A.; de Leeuw, S. W. *J. Phys. Chem. B* **2004**, *108*, 16139.

(18) Ye, A.; Shuai, Z.; Kwon, O.; Bredas, J. L.; Beljonne, D. *J. Chem. Phys.* **2004**, *121*, 5567.

(19) Fratiloiu, S.; Candeias, L. P.; Grozema, F. C.; Wildeman, J.; Siebbeles, L. D. A. *J. Phys. Chem. B* **2004**, *108*, 19967.

(20) Fratiloiu, S.; Grozema, F. C.; Siebbeles, L. D. A. *J. Phys. Chem. B* **2005**, *109*, 5644.

(21) Dudek, S. P.; Pouderoijen, M.; Abbel, R.; Schenning, A. P. H. J.; Meijer, E. W. *J. Am. Chem. Soc.* **2005**, *127*, 11763.

(22) Koizumi, Y.; Seki, S.; Acharya, A.; Saeki, A.; Tagawa, S. *Chem. Lett.* **2004**, *33*, 1290.

(23) Seki, S.; Yoshida, Y.; Tagawa, S.; Asai, K. *Macromolecules* **1999**, *32*, 1080.

(24) te Velde, G.; Bickelhaupt, F. M.; Baerends, E. J.; Guerra, C. F.; van Gisbergen, S. J. A.; Snijders, J. G.; Ziegler, T. *J. Comput. Chem.* **2001**, *22*, 931.

(25) Vosko, S. H.; Wilk, L.; Nusair, M. *Can. J. Phys.* **1980**, *58*, 1200.

(26) Jensen, F. *Introduction to computational chemistry*; John Wiley & Sons Ltd.: Chichester, UK, 1999.

(27) Becke, A. D. *Phys. Rev. A* **1988**, *38*, 3098.

(28) Perdew, J. P. *Phys. Rev. B* **1986**, *33*, 8800.

(29) Kong, J.; White, C. A.; Krylov, A. I.; Sherrill, D.; Adamson, R. D.; Furlani, T. R.; Lee, M. S.; Lee, A. M.; Gwaltney, S. R.; Adams, T. R.; Ochsenfeld, C.; Gilbert, A. T. B.; Kedziora, G. S.; Rassolov, V. A.; Maurice, D. R.; Nair, N.; Shao, Y.; Besley, N. A.; Maslen, P. E.; Korambath, J. P.; Baker, J.; Byrd, E. F. C.; van Voorhis, T.; Oumi, M.; Hirata, S.; Hsu, C.; Ishikawa, N.; Florian, J.; Warshel, A.; Johnson, B. G.; Gill, P. M. W.; Head-Gordon, M.; Pople, J. A. *J. Comput. Chem.* **2000**, *21*, 1532.

(30) Lee, C.; Yang, W.; Parr, R. G. *Phys. Rev. B* **1988**, *37*, 785.

(31) Dunning, T. H. *J. Chem. Phys.* **1989**, *90*, 1007.

(32) Runge, E.; Gross, E. K. U. *Phys. Rev. Lett.* **1984**, *52*, 997.

(33) Petersilka, M.; Gossmann, U. J.; Gross, E. K. U. *Phys. Rev. Lett.* **1996**, *76*, 1212.

(34) Belletete, M.; Beaupre, S.; Bouchard, J.; Blondin, P.; Leclerc, M.; Durocher, G. *J. Phys. Chem. B* **2000**, *104*, 9118.

(35) Cooper, R.; Thomas, J. K. *J. Chem. Phys.* **1968**, *48*, 5097.

(36) Schmidt, W. F.; Allen, A. O. *J. Phys. Chem.* **1968**, *72*, 3730.

(37) Gee, N.; Freeman, G. R. *Can. J. Chem.* **1992**, *70*, 1618.

(38) Shinsaka, K.; Freeman, G. R. *Can. J. Chem.* **1974**, *52*, 3495.

(39) Gorman, A. A.; Lovering, G.; Rodgers, M. A. J. *J. Am. Chem. Soc.* **1978**, *100*, 4527.

(40) Huang, S. S.-S.; Freeman, G. R. *J. Chem. Phys.* **1980**, *72*, 1989.

(41) Warman, J. M.; Infelta, P. P.; de Haas, M. P.; Hummel, A. *Chem. Phys. Lett.* **1976**, *43*, 321.

(42) Grozema, F. C.; Hoofman, R. J. O. M.; Candeias, L. P.; de Haas, M. P.; Warman, J. M.; Siebbeles, L. D. A. *J. Phys. Chem. A* **2003**, *107*, 5976.

(43) Burrows, H. D.; Seixas de Melo, J.; Forster, M.; Guntner, R.; Scherf, U.; Monkman, A. P.; Navaratnam, S. *Chem. Phys. Lett.* **2004**, *385*, 105.

(44) Burrows, H. D.; da G.Miguel, M.; Monkman, A. P.; Horsburgh, L. E.; Hamblett, I.; Navaratnam, S. *J. Chem. Phys.* **2000**, *112*, 3082.

(45) Jou, F. Y.; Dorfman, L. M. *J. Chem. Phys.* **1973**, *58*, 4715.

(46) Tran-Thi, T. H.; Koulkes-Pujo, A. M. *J. Phys. Chem.* **1983**, *87*, 1166.

(47) Baxendale, J. H.; Beaumond, D.; Rodgers, M. A. J. *Int. J. Radiat. Phys. Chem.* **1970**, *2*, 39.

(48) Dodelet, J.-P.; Freeman, G. R. *Can. J. Chem.* **1975**, *53*, 1263.
(49) Buxton, G. V.; Stuart, C. R. *J. Chem. Soc., Faraday Trans.* **1995**, *91*, 279.
(50) Schmidt, W. F.; Allen, A. O. *J. Chem. Phys.* **1970**, *52*, 2345.
(51) Shaede, E. A.; Kurihara, H.; Dorfman, L. M. *Int. J. Radiat. Phys. Chem.* **1974**, *6*, 47.
(52) Kira, A.; Nakamura, T.; Imamura, M. *J. Phys. Chem.* **1978**, *82*, 1961.
(53) Kira, A.; Imamura, M. *J. Phys. Chem.* **1978**, *82*, 1966.
(54) Tirapattur, S.; Belletete, M.; Leclerc, M.; Durocher, G. *J. Mol. Struct.* (*THEOCHEM*) **2003**, *625*, 141.
(55) Fesser, K.; Bishop, A. R.; Campbell, D. K. *Phys. Rev. B* **1983**, *27*, 4804.
(56) Furukawa, Y. *Synth. Met.* **1995**, *69*, 629.
(57) Thormann, T.; Rogojerov, M.; Jordanov, B.; Thulstrup, E. W. *J. Mol. Struct.* **1999**, *509*, 93.